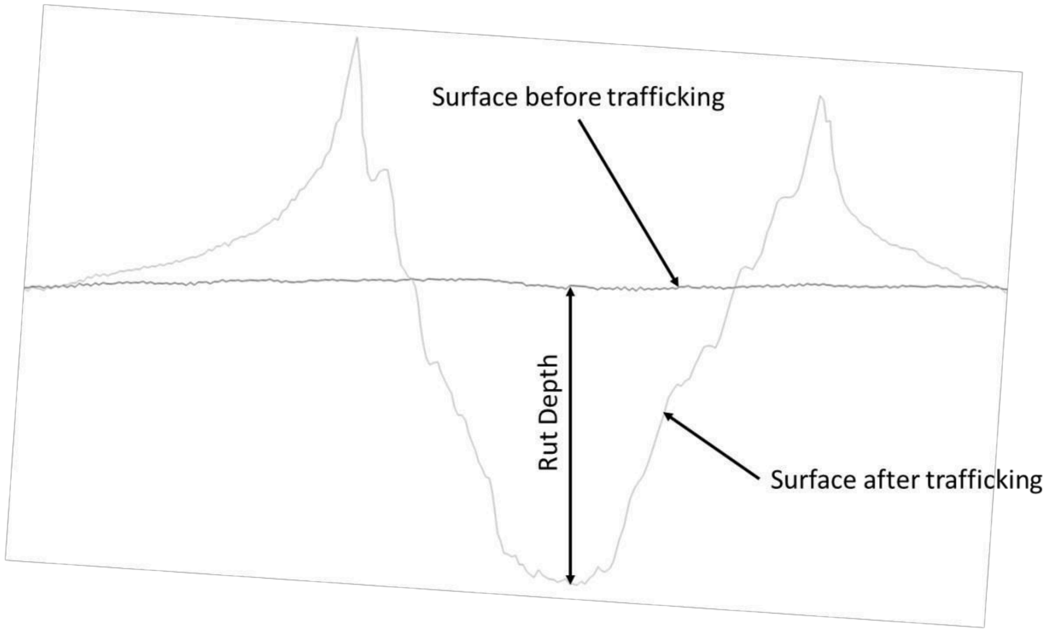

Figure 8. Cross-section of rut showing rut depth definition.

2.2 STATISTICAL APPROACH

Data were analyzed using a script that calculated the rut depth for stations 18 to 93 of each test section, which covers the center 25 feet of the test section. Rut depth according to Figure 8 was calculated as the difference between the elevation of the un-trafficked section of the pavement cross-section and the minimum elevation at each station. These rut depths were then used to calculate the mean and standard deviation of rut depth for each set of profile data. The equation used to calculate standard deviation was (Montgomery et al 1994):

$$s = \sqrt{\frac{\sum_{i=1}^{n} x_i^2 - \frac{(\sum_{i=1}^{n} x_i)^2}{n}}{n-1}}$$

3 RESULTS AND ANALYSIS

Standard deviation of rut depth is plotted against the applied number of wanders of traffic in Figure 9. As stated previously, each wander consists of 62 passes. Rut depth after each wander (application of 62 passes) is shown in Figure 10. Standard deviation of rut depth typically has a starting value of less than 0.1 inches and increases with trafficking. The average value of the standard deviation of rut depth is 0.093 inches. This implies that the 95% confidence interval around a single rut depth measurement is approximately plus or minus 0.18 inches, however, researchers are typically most interested in rut depth at failure. Using the regression equation shown on Figure 10, the expected standard deviation of rut depth on a pavement with a rut that is 1 inch deep is 0.110 inches. Confidence interval is calculated as (Montgomery et al 1994):

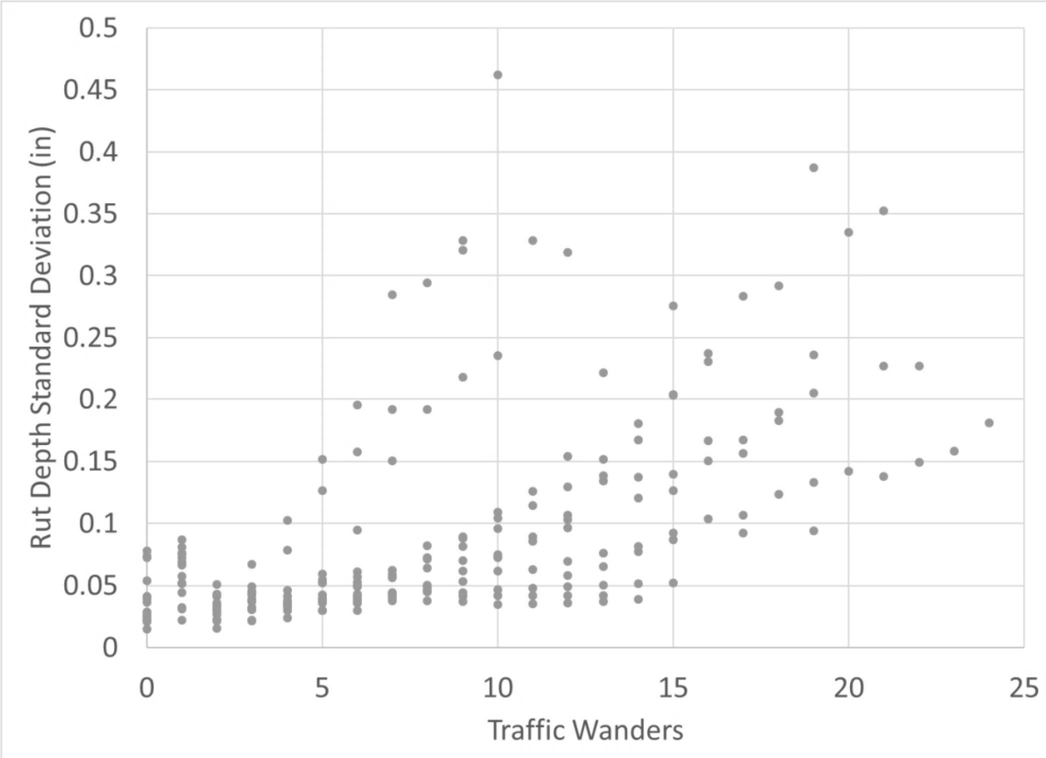

Figure 9. Standard deviation of rut depth by number of wanders for all sections.

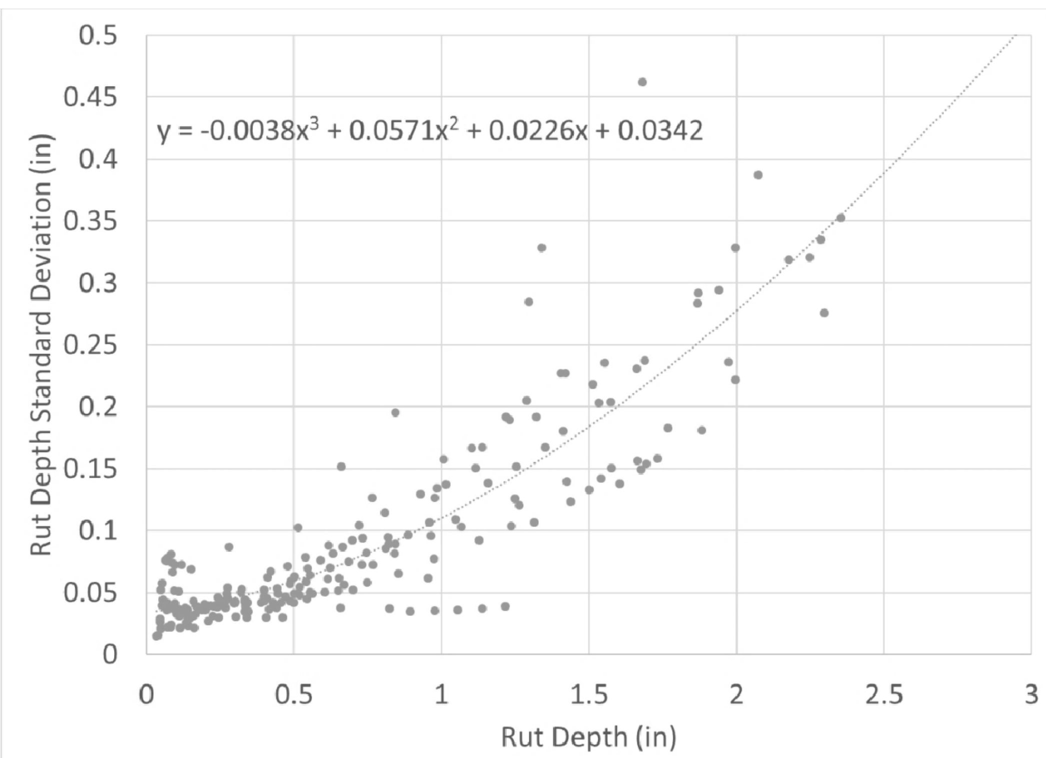

Figure 10. Standard deviation of rut depth by average rut depth.

$$\bar{x} \pm \frac{\left(z\alpha/_2\right)(s)}{\sqrt{n}}$$

If rut depth is determined from a single measurement, the 95% confidence interval at failure is $\bar{x}$±0.22 inches. This means that if rut depths are determined from a single measurement, the difference between two test sections needs to be nearly one-half an inch to be statistically significant. This can be reduced significantly by increasing n by measuring at multiple stations, as shown in Table 2.

The average standard deviation of rut depth for each test parameter of the experiment is listed in Table 3. Binder grade 76-22 exhibited a lower variability in rut depth than 64-22 binder and unheated pavements exhibited lower variability than pavements tested hot, which matched the researcher's expectations. WMA exhibited a higher variability than HMA, which was unexpected. Compaction of HMA is very dependent on the compaction temperature, but WMA has an additive mixed in at the plant and evenly distributed throughout the material to allow compaction at lower temperatures. Researchers expected this to result in a more uniform material and therefore lower variability in performance. Testing at high tire pressures resulted in decreased variability, which was also unexpected.

Table 2. Confidence interval for α=0.05 and s=0.110 inches for various sample sizes.

Number of Measurements (n)	95% Confidence Interval (in)
1	±0.216
2	±0.153
76	±0.025
110	±0.020

Table 3. Standard deviation by test parameter.

	Item 1			Item 2		
Parameter	**Item**	**s (in)**	**n**	**Item**	**s (in)**	**n**
Material	HMA	0.085	138	WMA	0.102	129
Tire Pressure	210psi	0.126	72	254psi	0.085	195
Binder Grade	76-22	0.090	183	64-22	0.102	84
Heating	Unheated	0.043	102	Heated	0.121	165

4 INTERPRETATION OF RESULTS AND CONCLUSIONS

The average value of the standard deviation of rut depth in the NAPMRC HVS-A test sections was 0.093 inches. This compares well with values reported from other studies. Standard deviation of rut depth correlated well to rut depth, increasing with rut depth. This likely explains the loose positive correlation between standard deviation of rut depth and traffic. Trafficking causes rutting, so as the trafficking causes the ruts to get deeper, the variability in rut depth increases. Because different materials rut at different rates under trafficking, the variability in rut depth of different materials also increases at different rates under trafficking. Variability in rut depth is not related to the absolute number of traffic cycles to which a pavement is exposed, but the depth of ruts in the pavement regardless of the number of traffic cycles necessary to cause the ruts.

The 95% confidence interval for mean rut depth as determined from a single measurement is approximately $\bar{x}\pm0.22$ inches. Determining the mean rut depth from multiple measurements of a laser profiler reduces this by an order of magnitude to approximately $\bar{x}\pm0.02$ inches. Rut depths used for performance modeling should be mean rut depths determined from laser profiler data.

ACKNOWLEDGEMENTS AND DISCLAIMER

The work described in this paper was supported by the FAA Airport Technology R&D Branch, Dr. Michel J. Hovan, Manager, and by Dr. Navneet Garg, Project Manager. The contents of the paper reflect the views of the authors, who are responsible for the facts and accuracy of the data presented therein. The contents do not necessarily reflect the official views and policies of the FAA. The paper does not constitute a standard, specification, or regulation.

REFERENCES

Byron, T., Gokhale, S., and Choubane, B. (2005). "Laser-Based Technology for Automated Rut Measurement in Accelerated Pavement Testing." *84th Annual Meeting of Transportation Research Board*, Transportation Research Board, Washington, DC, 1–17.

Epps. A. L., Ahmed, T., Little, D. C., and Hugo, F. (2001). *FHWA/TX-01/2134-1: Performance Prediction With The MMLS3 at Westrack*. Texas Department of Transportation, Austin, TX.

Gokhale, S., Choubane, B., Byron, T., and Tia, M. (2005). "Rut Initiation Mechanisms in Asphalt Mixtures as Generated Under Accelerated Pavement Testing." *Transportation Research Record: Journal of the Transportation Research Board*, Transportation Research Board of the National Academies, (1940), 136–145.

Harvey, J., Louw, L., Guada, I., Hung, D., and Scheffy, C. (1998). "Performance of CAL/APT Drained and Undrained Pavements Under HVS Loading." *Transportation Research Record: Journal of the Transportation Research Board*, (1615), 11–20.

Harvey, J. T., Louw, L., Guada, I., Hung, D., Prozzi, J., and Long, F. (1999). *CAL/APT Program: Test Results From Accelerated Pavement Test on Pavement Structure Containing Untreated Aggregate Base (AB) Section 501RF*. Sacramento, CA.

Harvey, J. T., Plessi, L., Long, F., Deacon, J., Guada, I., Hung, D., and Scheffy, C. (1997). *CAL/APT Program: Test Results from Accelerated Pavement Test on Pavement Structure Containing Asphalt Treated Permeable Base (ATPB) Section 500RF*. Sacramento, CA.

Hoffman, B. R. (2011). "Evaluation of the Automated Laser Rut Measurement System Used by the Ohio Department of Transportation." Master's Thesis, University of Ohio.

Montgomery, D.C. and G.C. Runger (1994). *Applied Statistics and Probability for Engineers*. John Wiley & Sons, New York.

Steyn, W. J. (2012). *NCHRP Synthesis 433: Significant Findings from Full-Scale Accelerated Pavement Testing*. Transportation Research Board, Washington, D.C.

Concrete Pavement Overload Test at the FAA's National Airport Pavement Test Facility

H. Yin[1] and D. R. Brill[2]

[1]Gemini Technologies, Inc., 3153 Fire Rd., Egg Harbor Township, NJ 08234. E-mail: hao.yin@gemitek.com
[2]Federal Aviation Administration, Airport Technology R&D Branch, William J. Hughes Technical Center, ANG-E262, Atlantic City International Airport, NJ 08405. E-mail: david.brill@faa.gov

Abstract

As part of Construction Cycle 8 (CC8) at the National Airport Pavement Test Facility (NAPTF), the Federal Aviation Administration (FAA) is conducting full-scale tests on an unbonded concrete overlay test pavement. In preparation for receiving the portland cement concrete (PCC) overlay, the relatively thin existing PCC surface layer was damaged by simulated heavy aircraft gear traffic applied by the NAPTF test vehicle. Data obtained from this initial trafficking phase will be used by the FAA to evaluate current ICAO standards for allowable aircraft overloads on rigid pavements. This paper discusses various aspects of the overload testing, including: pavement design, construction, and instrumentation, PCN evaluation, overload test procedures, and traffic test results. The difference in applied coverages to failure was used to evaluate the effect of the overload. In addition, the cause and failure mechanism of observed distresses were discussed. This overload test generated a unique full-scale test data set, which be used by the FAA to evaluate current ICAO standards for allowable aircraft overloads on rigid pavements.

INTRODUCTION

The Aircraft Classification Number–Pavement Classification Number (ACN–PCN) system of rating airport pavements is designated by the International Civil Aviation Organization (ICAO) as the only approved method for reporting pavement strength. The concept of ACN-PCN method is structured so that a pavement with a given PCN value can support unrestricted operations of an aircraft that has an ACN value equal to or less than the PCN value. FAA Advisory Circular (AC) 150/5335-5C (FAA 2014) provides guidance on reporting airport pavement strength and is mandatory for all projects funded with federal grant money through the AIP program. ICAO Annex 14 (ICAO 2013) establishes overload criteria for both rigid and flexible airport pavements. The ICAO criteria recognize that airport operators should have flexibility to allow occasional operations by aircraft whose ACN exceeds the assigned PCN, and that as long as these operations do not become regular, the additional damage they cause is likely to be manageable. As stated in AC 150/5335-5C, Appendix D, "With the exception of massive overloading, pavements do not suddenly or catastrophically fail. As a result, occasional minor overloading is acceptable with only limited loss of pavement life expectancy and relatively small acceleration of pavement deterioration." According to ICAO Annex 14, occasional movements on rigid pavements by aircraft with ACN values not exceeding 5 percent above the reported PCN "should not adversely affect the pavement."

RESEARCH SIGNIFICANCE

The objective of the research effort was to develop new, rational overload criteria for airfield rigid pavements. Although the current ICAO overload criteria represent a "reasonable balance between operational flexibility and the need to avoid undue damage to pavements," (Defence Estates 2011) they are still somewhat conservative and unsupported by empirical data. For example, limited Construction Cycle 6 (CC6) test data at the FAA's NAPTF demonstrated that a one-time application of rupture load (i.e., equal to or exceeding the slab strength) did not necessarily shorten pavement life (Brill 2013). Ideally, allowable overload criteria would be linked to the cumulative damage factor (CDF), which would then allow individual overloads to be related to consumed life.

TEST PAVEMENT AND INSTRUMENTATION

The FAA is conducting full-scale tests on an unbonded concrete overlay test pavement, designated CC8, at the NAPTF. In preparation for receiving the PCC overlay, the relatively thin existing PCC surface layer was damaged by simulated heavy aircraft gear traffic applied by the NAPTF test vehicle. The overload test area has two test items (north and south), is 60 feet long by 60 feet wide, and consists of twenty 12×12-ft. slabs, as shown in Figure 1. The pavement structure is 9-inch thick concrete slabs on an 11-inch thick granular base, on a prepared clay subgrade. Based on plate load tests, the modulus of subgrade reaction (*k*-value) is approximately 110 pci on the north test item, and 131 pci on the south test item. Since no stabilized base is present, this rigid pavement structure may be considered representative of a non-hub or general aviation facility, i.e., not intended to handle heavy aircraft loads. All longitudinal joints are doweled and all dowels are 0.75 inches in diameter. However, the transverse joints are not doweled.

Prior to the placement of the surface P-501 layer, all subgrade, subbase and concrete slab instrumentation had to be installed. The selection of gages was based on reliability, accuracy, price, and ease of handling at the construction site. Instrumentation details are given in Figure 1. Vertical movement of slab corners relative to the base was monitored by eddy current sensors (ECS) that were intended to operate in both static mode (to monitor long-term upward movement of slab corners) and dynamic mode (to record transient responses to vehicle loads). Pairs of embedded strain gages were installed along longitudinal and transverse edges of eight slabs to measure strain responses near the top (odd numbered gages) and bottom (even numbered gages) of the instrumented slabs. Rebar chairs ensured that strain gages were set at the proper height (1 in. above the slab bottom and 1 in. below the slab top). Thermocouple trees were installed in two slabs to monitor slab temperature gradients. Each tree consists of three thermocouples to measure temperature at the bottom, middle and top of the slab.

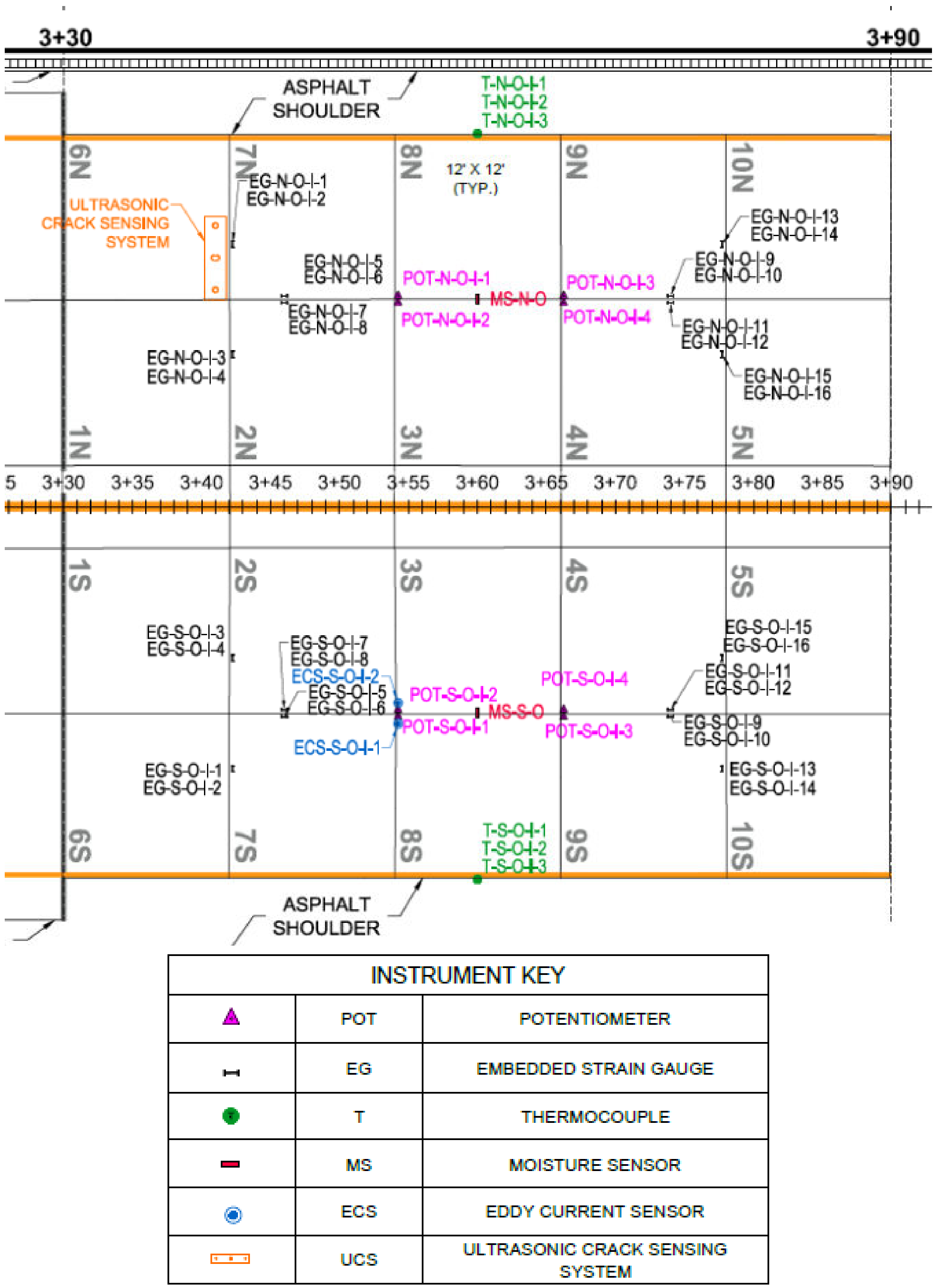

Figure 1. General construction and instrumentation layout. Stationing is shown in hundreds of feet.

TEST PLAN

A test plan was developed to evaluate the effect of limited overload traffic on overall rigid pavement life. Because of the small test area available (two 24 × 60 ft. test items) the number of variables that could be considered was small. Only one of the two identical test items would receive a series of controlled overloads, based on a percentage of the computed PCN. Both test items would then be trafficked to a predefined failure condition, defined as a structural condition index (SCI) of approximately 80. The difference in applied coverages to failure will then be indicative of the effect of the initial overload. The specific steps are as follows:

1. Compute a PCN for the test pavement, using the design assumptions and the method of FAA AC 150/5335-5C (COMFAA 3.0). The PCN assumes that the design traffic is a dual (D) gear aircraft and that a reasonable number of passes to failure in this case is between 10,000 and 15,000. Test traffic will be applied using a wander pattern consisting of 66 passes on 9 discrete tracks, representing an assumed normal lateral distribution around the nominal centerline. The selected wander pattern is illustrated in Figure 2.
2. Once the PCN is established, develop a series of overloads, based on dual tandem (2D) aircraft loads, with ACNs between 5% and 25% above the declared PCN.
3. After conducting initial baseline measurements of pavement properties and verifying the responses of in-pavement sensors, run one complete wander pattern (see step 1) on both test items. Check strain responses under the wheel path and compare with the thickness design.
4. On the south test item only, apply overload passes using the same wander pattern as in step 3, but using a 2D gear configuration with accordingly increased wheel loads. Apply overloads in increasing increments until either (a) observation of a crack visually or by strain gage analysis, or (b) completion of a full wander pattern at the 25% overload level.
5. Traffic both test items normally until failure is observed on one of the test items. Continue trafficking the other (non-failed) test item until both test items are at the same condition, as measured by the structural condition index (SCI).

A key element of this test plan is continual pavement condition monitoring. This is important because the follow-on experiment in CC8, involving PCC-on-rigid overlays, will require a specific value of SCI as a starting point for the pavement receiving the overlay (Yin 2013). It is important the overload test traffic not impart too much damage. Throughout the traffic testing, the structural performance of test pavement was monitored and quantified by means of the SCI. SCI is a modification of the Pavement Condition Index (PCI) for Airports (rigid) method following ASTM D 5340 (ASTM 2012). Like PCI, SCI is based on visual inspection of the pavement surface and identification of standard distresses. The difference is that in the SCI only distresses related to structural loading are counted, while environmental and construction/material-related distresses are disregarded. In the field, pavements are divided into "sample units," and a subset of sample units is then randomly selected for inspection. Due to the small size of test area, south and north test item were considered to constitute a separate sample unit, and 100% inspection (i.e., of 10 slabs) was performed.

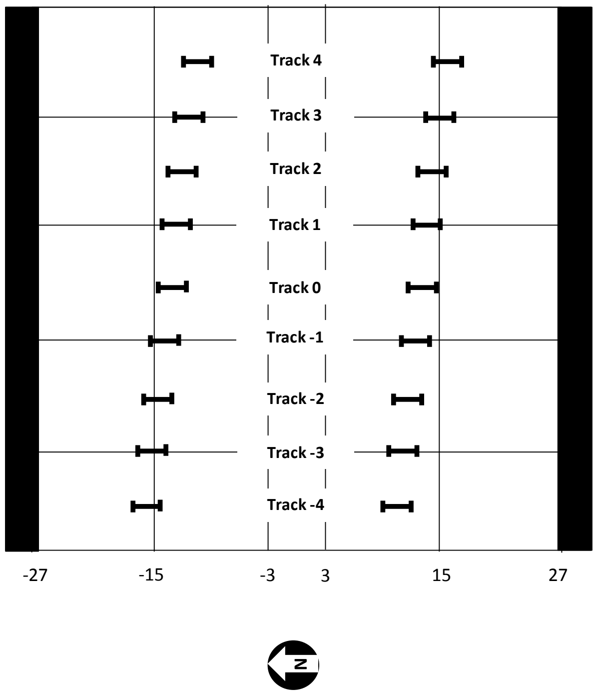

Track #	Carriage Centerline Location, ft	
	North	South
-4	-15.662	8.838
-3	-14.809	9.691
-2	-13.956	10.544
-1	-13.103	11.397
0	-12.250	12.250
1	-11.397	13.103
2	-10.544	13.956
3	-9.691	14.809
4	-8.838	15.662

Figure 2. Wander pattern.

An evaluation of the test pavement was performed using FAARFIELD 1.4, assuming the following structure: 9 in. PCC, FAA Item P-501; 11 in. aggregate base, FAA Item P-154, average subgrade k = 120 pci. Concrete strength was taken as R = 650 psi, based on the average flexural strength (ASTM C78) of concrete beams cast at the time of construction and tested at the start of traffic. Assuming that the design traffic load is a dual (D) aircraft gear with 20,000 lbs. per wheel (corresponding to an aircraft gross weight of 84,211 lbs.), FAARFIELD predicts total lifetime traffic of 10,405 passes. This life prediction is based on the FAARFIELD 1.4 rigid pavement failure model and a computed maximum edge stress (with assumed load transfer) of 445 psi.

The PCN was determined using the program COMFAA 3.0 and the method of AC 150/5335-5C. Assuming an improved top-of-base k-value (210 pci) based on the contribution of the 11 in. P-154 layer, for the above lifetime traffic COMFAA gives a PCN value of 21.1 on a “C” subgrade. The computed ACN for the NAPTF dual gear at 20,000 lbs. per wheel and 220 psi tire pressure is 20.4 on “C” subgrade, which is less than the PCN, as expected. Therefore, the PCN was established as 21/R/C, and an initial schedule of overloads based on this PCN was established as in Table 1. ACNs were determined for the NAPTF 2D gear using the COMFAA 3.0 program. Note that actual percent increases over the declared PCN differ from the whole numbers, because it is only possible to control the target wheel load to increments of 500 lbs.